

EPC GaN Transistor Application Readiness: Phase One Testing



Yanping Ma PhD, Director of Quality and Reliability, Efficient Power Conversion Corporation

Efficient Power Conversion Corporation's (EPC) enhancement mode Gallium Nitride (GaN) power transistors offer performance well beyond the realm of silicon-based MOSFETs. Standard power converter topologies can greatly benefit from the added performance and realize improved efficiency while maintaining the simplicity of older designs.

Although similar to standard power MOSFETs, enhancement mode GaN transistors are a relatively new technology. Operating life information is not yet at the level available to users of silicon power MOSFETs. EPC's risk-reduction results to date include the placement of over 380 devices, at their maximum operating ratings on a wide variety of stress tests. Over 275,000 total device hours support our product's readiness for commercial use. The conversion of power MOSFET-based systems can begin with acceptable levels of risk.

In this paper, the suitability for reliable and commercial use of EPC technology will be addressed in detail.

GaN OVERVIEW

The fundamental properties of GaN make it an ideal starting material for high power transistors. Some of these properties are derived from the crystal's wide band-gap of 3.4 eV. This wide band-gap creates an extremely high electric breakdown field (about 10 times of silicon), making GaN an outstanding material for high voltage transistors and for operation at elevated temperatures. The electron density resulting from the polarization-induced field in the GaN structure is very high ($\sim 10^{13}/\text{cm}^2$). The high two-dimensional electron gas (2DEG) density and high electron mobility make GaN high electron mobility transistors (HEMTs)¹ very

attractive for low on-state resistance power transistors with high breakdown voltage and high current density capability.

GaN Devices Have Been the Subject of Intense Research for the Past Decade

Research and development projects sponsored by the Defense Advanced Research Agency (DARPA) including teams from Triquint, Raytheon and Northrop Grumman have resulted in estimated transistor lifetime using single failure mode Arrhenius elevated temperature testing of >100,000 hours at a junction temperature of 150°C. This represents a five order of magnitude increase in transistor lifetime,

taking GaN from a laboratory novelty to being able to compete with mature technologies^{2,4}. Commercial GaN HEMTs are already available for the RF and microwave markets from companies such as Nitronex³, RFMD⁴, and Eudyna⁵.

Although the focus of research and development has been depletion-mode or d-mode (normally-on) HEMTs, enhancement-mode or e-mode (normally-off) HEMTs are strongly preferred. Enhancement-mode (normally-off) HEMTs offer safer operation, greater simplicity of circuit design, and lower energy consumption. There are numerous examples in the literature regarding enhancement-mode GaN HEMTs (HEMT can be used interchangeably with HFET, heterostructure field effect transistors) including but not limited to:

- Recessed etching of the AlGaIn barrier in conjunction with a Schottky gate electrode³⁰
- Fluoride-based plasma treatment of the gate³¹
- E-mode HFET using p-n junction gate contact⁶
- E-mode HFET utilizing conductivity modulation^{9,10}

EPC PRODUCT INTRODUCTION

Efficient Power Conversion enhance-mode HFETs were commercialized in June of 2009. Figure 1 shows a schematic structure of an EPC device which is similar to a lateral DMOS silicon device and fabricated on silicon substrates, employing standard silicon processes. The cost of EPC products is therefore comparable to silicon technologies¹¹.

During 2009, EPC introduced ten part numbers covering 40, 60, 100, 150 and 200 volt enhancement-mode GaN power transistors. The voltage ratings, maximum $R_{DS(on)}$, and

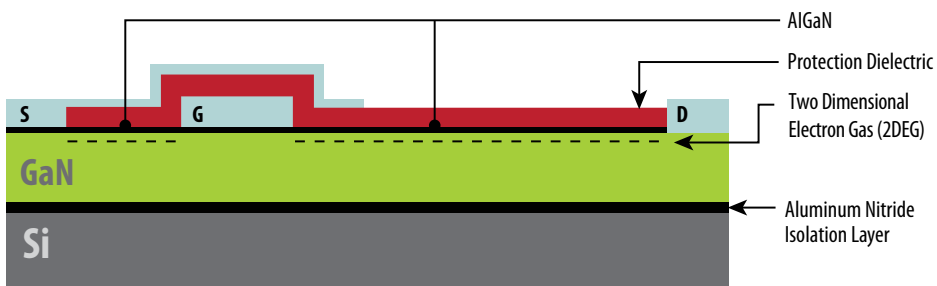


Figure 1: GaN on silicon devices have a very simple structure similar to a lateral DMOS device and are built in a standard CMOS foundry

product dimensions are listed in Appendix I. EPC’s GaN transistors are lateral devices with all three terminals: gate, drain, and source on the front side of the chip. The active device is isolated from the substrate and fully encapsulated by passivation layers on the front side as shown in Figure 2. This configuration allows EPC’s GaN transistors to be used as bare die without additional packaging²⁸. The advantages include: the elimination of plastic packages and the related performance issues, improved reliability, and cost reduction. EPC GaN transistors employ wafer-level solder line-grid-arrays as shown in Figure 3.

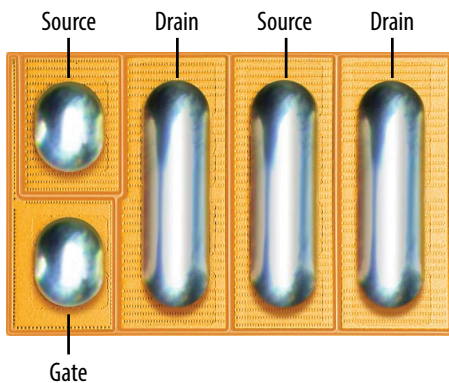


Figure 3: Front side view of EPC 1014, 40 V, 16 mΩ GaN transistor showing the solder line-grid-array bump design with alternating source and drain solder bars.

RELIABILITY PROGRAM OVERVIEW

The conversion of Power MOSFET-based systems to enhancement-mode GaN technology requires evidence of reliable performance. In Phase One, EPC stressed more than 380 devices for a total of more than 275,000 hours under conditions similar to power MOSFET reliability stress testing.

“Dynamic $R_{DS(on)}$ ”, specifically those conditions causing minimal shifting in device resistance, is extensively discussed in the literature and was a particular focus of the EPC Phase One reliability program¹²⁻²⁷. EPC’s devices have been designed to mitigate dynamic $R_{DS(on)}$ and data show significantly greater stability than devices reported in the literature.

Dynamic $R_{DS(on)}$

Dynamic $R_{DS(on)}$ is a phenomenon whereby a device’s on-resistance increases after being subjected to a drain bias. The magnitude of the increase depends on the drain-side gate edge electric field, under which electrons are accelerated and a small number remained trapped in the

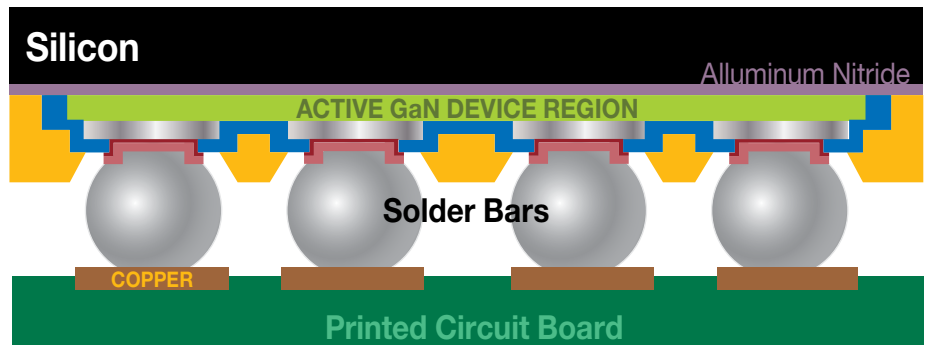


Figure 2: GaN on silicon can be used as a “flip chip.” The active device is isolated from the silicon substrate and can be completely encapsulated prior to singulation. When compared to plastic packages, this design reduces cost and requires less space.

EPI layer, or at the EPI surface. As the trapped electrons deplete the 2DEG, $R_{DS(on)}$ is increased. The higher the drain pre-bias voltage, the higher the $R_{DS(on)}$ becomes post-bias. Over time, the trapped electrons de-trap (relax) and $R_{DS(on)}$ gradually returns to the pre-bias value.

Several companies and institutions have reported suppression of dynamic $R_{DS(on)}$ by surface passivation^{20,21}. Proper field-plating can also reduce the peak electric field, thereby suppressing dynamic $R_{DS(on)}$ ¹⁷. It was reported that dynamic $R_{DS(on)}$ was much improved with GaN devices built on conductive silicon substrates compared to GaN devices built on non-conductive sapphire substrates²⁹. This improvement is due to the conductive substrate acting as a field plate on the back side. With GaN on a conductive substrate, dynamic $R_{DS(on)}$ was reported being influenced by the GaN EPI layer thickness.

EPC products use an optimized EPI structure and EPI thickness on conductive silicon substrates to minimize dynamic $R_{DS(on)}$. The EPI surface is passivated with a high quality Si_3N_4 layer. Field plate structures are also optimized. Figure 4 shows an example comparing field-plate structure A, B, and C that were studied during EPC product

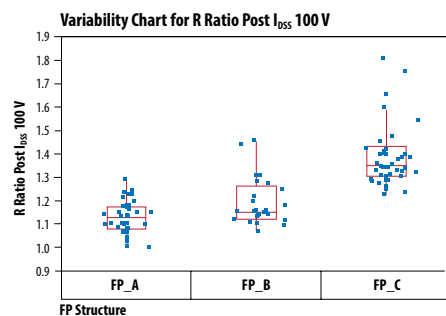


Figure 4: Field plate has big impact on dynamic $R_{DS(on)}$. An example is shown comparing field-plate structure A, B, and C that were studied during product development.

development. Field-plate structure A is superior in terms of dynamic $R_{DS(on)}$.

Dynamic $R_{DS(on)}$ was evaluated on a TESEEC tester. $R_{DS(on)}$ was measured pre and post stress whilst the drain-source voltage was stepped from low

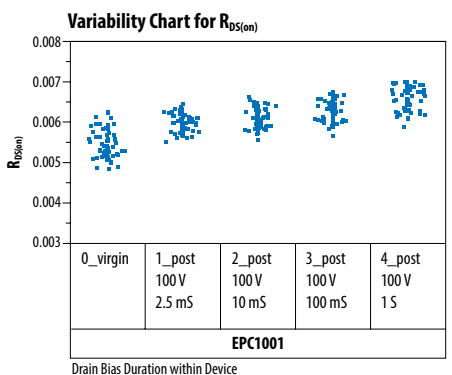


Figure 5: $R_{DS(on)}$ values after 100 V bias for various durations.

voltage to 30% above the rated maximum drain-source voltage. The effect of drain bias duration was also evaluated. Figure 5 shows $R_{DS(on)}$ values after 100 V bias for various durations. Increasing drain bias duration from 2.5 mS to 1 Sec results in minimal increase in $R_{DS(on)}$.

The $R_{DS(on)}$ values post various drain biases for duration of 2.5 mS are shown in Figures 6, Figure 7, and Figure 8 for 40 V, 100 V, and 200 V product, respectively. Two device types are shown in each figure for each of the voltage ratings. The 40 V devices, EPC1014 and EPC1015, were biased to 40 V, 48 V and 52 V sequentially. The 100V devices, EPC1001 and EPC1007, were biased to 60 V, 100 V, and 130 V sequentially. The 200 V devices, EPC1010 and EPC1012, were biased to 100 V, 200 V, and 260 V sequentially. The degree of dynamic $R_{DS(on)}$ was similar for all product types. The increase in $R_{DS(on)}$ for the main population was approximately 10% with a tail at higher or lower values.

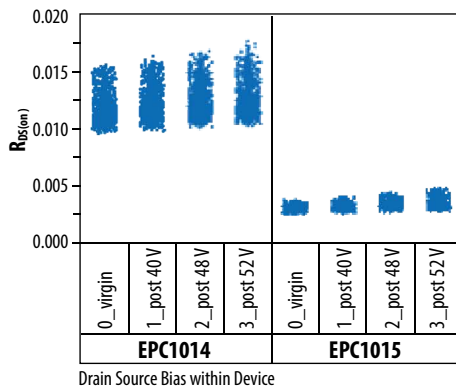


Figure 6: The $R_{DS(on)}$ values post various drain biases are shown for EPC1014 and EPC1015, the two 40 V products.

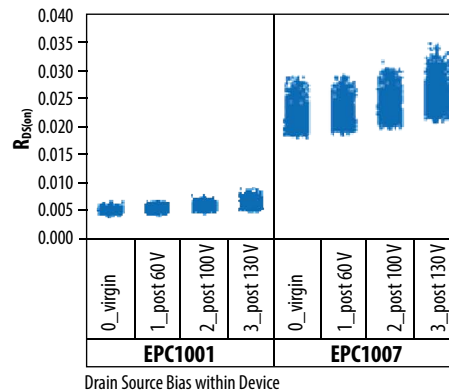


Figure 7: The $R_{DS(on)}$ values post various drain biases are shown for EPC1001 and EPC1007, the two 100 V products.

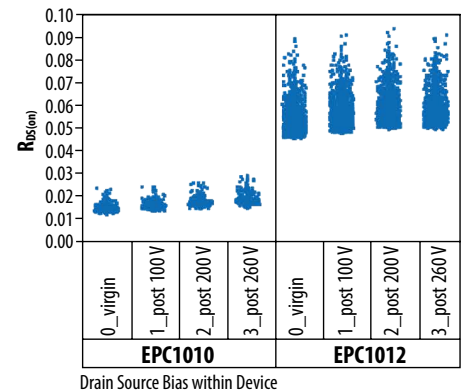


Figure 8: The $R_{DS(on)}$ values post various drain biases are shown for EPC1010 and EPC1012, the two 200 V products.

RELIABILITY TESTING OVERVIEW AND RESULTS

Long term stability under high drain-source bias was evaluated by subjecting devices to DC voltage equal to the maximum drain-source rated voltage and temperature (high temperature reverse bias, or HTRB). Gate reliability was evaluated by subjecting devices to various gate stresses at elevated temperature (high temperature gate bias, or HTGB). Environmental reliability was evaluated with temperature cycling (TC) and temperature-humidity-with-bias (THB). Devices were also subjected to operating life tests involving devices in actual power supplies running at high voltage and high current.

A list of the reliability tests performed, the applicable standards, the device types evaluated, and the stress conditions are listed in Appendix II. All devices tested were soldered onto Arlon 85N printed circuit boards.

High Temperature Reverse Bias Test (HTRB)

The impact of high drain bias on device parameters, applied for long periods of time, was evaluated with maximum rated drain-source bias applied at an ambient temperature of 125°C. Whereas there were no parametric failures out of the parts tested, there was some degree of dynamic $R_{DS(on)}$ post stress test (A 20% increase in $R_{DS(on)}$ was observed for some devices).

All electric parameters remained relatively constant throughout the entire stress period of 1000 hours for EPC1001 and EPC1014. Appendix IV graphically presents the stability of various device parameters during test.

High Temperature Gate Bias Test (HTGB)

The gate stability of EPC GaN transistors was evaluated under various gate bias conditions at 5 V, 5.4 V, and 6 V at 125°C. EPC1001 parts were used for each of the three tests. At 5 V_{GS} and 5.4 V_{GS} bias, all device electric parameters stayed relatively constant over the entire burn-in period of 1000 hours. It was observed though that the drain leakage increased with 6 V_{GS} bias. Five parts showed higher than the datasheet limit at the 168 hours pulling point (Appendix III*). These parts were put back on burn-in, and will be analyzed after the stress test is finished. Complete test results are presented in Appendix V.

Temp Cycle (TC)

Temperature cycling was conducted on EPC1001, a large device, and on EPC1014, a small device. These two part numbers have different bump designs and were used to check the bump joint reliability. Parts were all mounted on Arlon 85N printed circuit board material. Temperatures varied between -40°C to 125°C at a rate of two cycles per hour. No on-state resistance degradation was observed over the stress period of 1000 cycles. All electrical parameters remained constant during stress. Complete test results are shown in Appendix VI.

Temperature Humidity Bias Test (THB)

Device performance was also characterized with temperature and humidity with drain-source bias (THB). THB tests were conducted at 85°C and with 85% relative humidity. EPC1014 was on test with drain biased to the rated 40 volt.

At time of this writing, parts have completed 500 hours stress, and are continuing on test for 1000 hours. All device electric parameters remained relatively constant over the stress period. Complete test results are shown in Appendix VII.

Power Supply Operating Life Test

To demonstrate the performance of the GaN transistors in-circuit, and to test the reliability under high-stress operating life, EPC built 48 V to 1 V power supply boards using a “buck converter” topology (see figure 9). For the burn-in test, EPC1001 (100 V, 7 mΩ) transistors were used for both the control transistor and rectifier switches. This kind of test is particularly useful because, in a standard “buck” topology DC-DC converter operated at the high V_{IN}/V_{OUT} ratio of 48 V to 1 V, the control transistor is turned ON at a very low duty cycle (~2%). Conversely, the rectifier transistor is turned ON with a very high duty cycle (~98%). This test therefore stresses devices both at high drain-source voltage and high drain current under actual, fast-switching conditions. The converter was operated at 48 V input voltage, 1 V output voltage, 10 A output current, and at a switching frequency of 250 kHz. The circuit efficiency was measured at time-zero hour, 24, 48, 72, 168, 500, 1000, and 1200 hours. The normalized efficiency vs. burn-in hours is plotted in Figure 9(a), and the power supply test circuit is shown in Figure 9(b). The efficiency of all the power supply boards stayed virtually unchanged over the entire burn-in period.

FUTURE WORK

EPC has plans for a much broader and deeper study of the reliability of enhancement mode GaN power transistors. In Phase 2, EPC will complete the 1000 hour/1000 cycle testing on all product types. Further work will also be done to develop acceleration factors and models that allow users to determine suitability for various applications beyond basic commercial use.

Dynamic $R_{DS(on)}$ will continue to be investigated with the goal of further minimizing this characteristic of EPC GaN devices.

EPC will convert to lead free solder in the second half of 2010. This conversion will be accompanied by additional testing at 150°C to verify this change does not degrade device characteristics under stress. At that time, EPC will also conduct temperature cycling tests on a wide variety of substrate materials to validate compatibility.

SUMMARY

EPC's enhancement mode Gallium Nitride transistors bring tremendous performance and size advantages over silicon power MOSFETs. These advantages can be used to improve system efficiency, reduce system cost, reduce size, or a combination of all three. Because EPC's products were designed as power MOSFET replacements, designers can use their existing building blocks, skills and knowledge with only minor changes. Reliability testing has also demonstrated that the technology is now ready for general commercial use.

The future of GaN transistors is now.

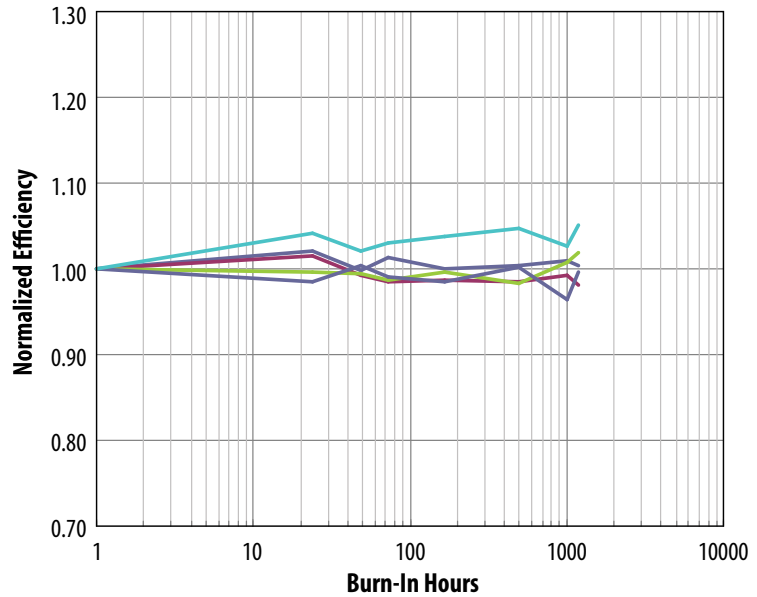


Figure 9(a): Power supply life test using EPC1001 at 30°C and 10 A. The normalized converter efficiency was plotted over 1200 hours of operating life.

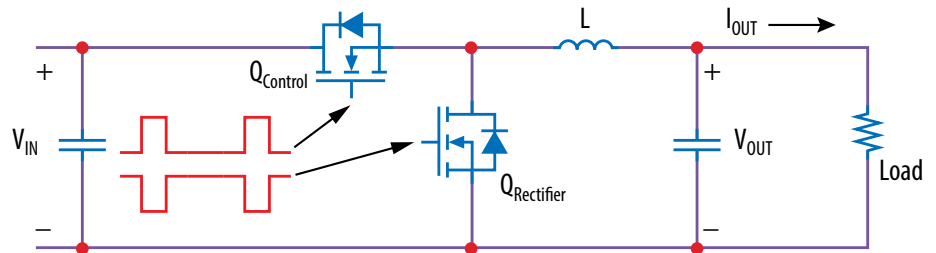


Figure 9(b): Power supply test circuit

References

1. M. Asif Khan, A. Bhattarai, J.N. Kuznia, and D.T. Olson, "High Electron Mobility Transistor Based on a GaN-AlxGa1-xN Heterojunction," *Appl. Phys. Lett.*, vol. 63, no. 9, 1993, pp. 1214-1215.
2. M.J. Rosker, "The Present State of the Art of Wide-Bandgap Semiconductors and Their Future," in *Proc. IEEE Radio Freq. Integr. Circuit Symp.*, 2007, pp. 159-162.
3. <http://www.nitronex.com>
4. <http://ir.fmd.com/releasedetail.cfm?ReleaseID=412122>
5. <http://www.mwrf.com/Article/ArticleID/13434/13434.html>
6. X. Hu, J. Simin, J. Yang, M. Asif Khan, R. Gaska, and M.S. Shur, "Enhancement Mode AlGaIn/GaN HFET with Selectively Grown PN Junction Gate," *Electronics Letters*, 2000, vol. 36, no. 8, pp. 753-754.
7. N. Tsuyuchi, K. Nagamatsu, Y. Hirose, M. Iwaya, S. Kamiyama, H. Amano, and I. Akasaki, "Low-Leakage-Current Enhancement-Mode AlGaIn/GaN Heterostructure Field-Effect Transistor Using p-Type Gate Contact," *Jpn. J. Appl. Phys.*, vol. 45, 2006, pp. L319-L321.
8. T. Fujii, N. Tsuyukuchi, M. Iwaya, S. Kamiyama, H. Amano, and I. Akasaki, "High on/off Ratio in Enhancement-Mode AlxGa1-xN/GaN Junction Heterostructure Field-Effect Transistors with p-Type GaN Gate Contact," *Jpn. J. Appl. Phys.*, vol. 45, no. 39, 2006, pp. L1048-L1050.
9. Y. Uemoto, M. Hikita, H. Ueno, H. Matsuo, H. Ishida, M. Yanagihar, T. Ueda, T. Tanaka, and D. Ueda, "Gate Injection Transistor (GIT) – A Normally-off AlGaIn/GaN Power Transistor Using Conductivity Modulation," *IEEE Transactions on Electron Devices*, vol. 54, no. 12, 2007, pp. 3393-3399.
10. Y. Uemoto, T. Ueda, T. Tanaka, D. Ueda, "Recent Advances of High Voltage AlGaIn/GaN Power HFETs," in *Proc. of SPIE Vol. 7216, 721606*, 2009, pp.1-11.
11. A. Lidow, "Is it the End of the Road for Silicon in Power Conversion?" *CIPS 2010 Conference Proceedings*, March 2010, Nurnberg, Germany.
12. W. Saito, M. Kuraguchi, Y. Takada, K. Tsuda, T. Doman, I. Omura, and M. Yamaguchi, "380 V/1.9A GaN power-HEMT: Current collapse phenomena under high applied voltage and demonstration of 27.1 MHz class-E amplifier," in *IEDM Tech. Dig.*, 2005, pp. 597-600.
13. S. Singhal, J.C. Roberts, P. Rajagopal, T. Li, A.W. Hanson, R. Therrien, J.W. Johnson, I.C. Kizilyalli, K.J. Linthicum, "GaN-on-Si failure mechanisms and reliability improvements," in *Proc. IEEE Int. Rel. Phys. Symp.*, 2006, pp. 95-98.
14. S. Singhal, T. Li, A. Chaudhari, A.W. Hanson, R. Theerien, J.W. Johnson, W. Nagy, J. Marquart, P. Rajagopal, J.C. Roberts, E.L. Piner, I.C. Kizilyalli, K.J. Linthicum, "Reliability of Large Periphery GaN-on-Si HFETs," *Microelectronics Reliability* 46, 2006, pp. 1247-1253.
15. P. Saunier, C. Lee, A. Galistreri, D. Dumka, J. Jimenez, H.Q. Tserng, M.Y. Kao, P.C. Chao, K. Chu, A. Souza, I. Eliashevich, S. Guo, J. del Alamo, J. Joh, M. Shur, "Progress in GaN Performances and Reliability," in *Proc. Device Res. Conf.*, 2007, pp. 35-36.
16. G. Meneghesso, G. Verellesi, F. Danesin, F. Rampazzo, F. Zanoni, A. Tazzoli, M. Meneghini, and E. Zanoni, "Reliability of GaN high-electron-mobility transistors: state of the art and perspectives," *IEEE Transactions on Device and Materials Reliability*, vol. 8, no. 2, 2008, pp. 332-343.
17. W. Saito, T. Nitta, Y. Kakiuchi, Y. Saito, K. Tsuda, I. Omura, and M. Yamaguchi, "On-Resistance Modulation of High Voltage GaN HEMT on Sapphire Substrate Under High Applied Voltage," *IEEE Electron Device Letters*, vol. 28, no. 8, 2007, pp. 676-678.
18. D. Marcon, A. Lorenz, J. Derluyn, J. Das, F. Medjdoub, K. Cheng, S. Degroote, M. Leys, R. Mertens, M. Germain, and G. Borghs, "GaN-on-Si HEMT stress under high electric field condition," *Phys. Status Solidi C*, vol. 6, 2009, pp. S1024-S1028.
19. R. Vetry, N.Q. Zhang, S. Keller, U.K. Mishra, "The impact of surface states on the DC and RF characteristics of AlGaIn/GaN HFETs," *IEEE Transactions on Electron Devices*, vol. 48, no. 3, 2001, pp. 560-566.
20. L. Ma, Y. Wang, T.Y. Guo, J. Lu, Z.B. Hao, Y. Luo, and Z.P. Yu, "Trap Related Current Collapse Effects in GaN HEMTs," *IEEE Conf. on Electron Devices and Solid State Circuits*, 2005, pp. 795-798.
21. T. Mizutani, Y. Ohno, M. Akita, S. Kishimoto, and K. Maezawa, "A Study on Current Collapse in AlGaIn/GaN HEMTs Induced by Bias Stress," *IEEE Transactions on Electron Devices*, Vol. 50, No. 10, 2003, pp. 2015-2020.
22. L. Shen, S. Heikman, B. Moran, et al., "AlGaIn/GaN High-Power Microwave HEMT," *IEEE Electron Device Letters*, vol. 22, 2001, pp.457-459.
23. Y.C. Chou, D. Leung, I. Smorchkova, M. Wojtowicz, R. Grundbacher, L. Callejo, Q. Kan, R. Lai, P.H. Liu, D. Eng, A. Oki, "Degradation of AlGaIn/GaN HEMTs Under Elevated Temperature Life testing," *Microelectronics Reliability*, vol. 44, 2004, pp. 1033-1038.
24. N. Shgaier, M. Trabelsi, N. Yacoubi, J.M. Bluet, A. Soufi, G. Guillot, C. Gaquiere, J.C. DeJaeger, "Traps Centers and Deep Defects Contribution in Current Instabilities for AlGaIn/GaN HEMTs on Silicon and Sapphire Substrates," *Microelectronics Journal* 37, 2006, pp. 363-370.
25. J. Joh, and J. del Alamo, "Mechanism for Electrical Degradation of GaN High-Electron Mobility Transistors," in *IEDM Tch. Dig.*, 2006, pp. 415-418.
26. S.Y. Park, C. Floresca, U. Chowdhury, J.L. Jimenez, C. Lee, E. Beam, P. Saunier, T. Balistreri, M.J. Kim, "Physical Degradation of GaN HEMT Devices Under Drain Bias Reliability Testing," *Microelectronics Reliability*, vol. 49, 2009, pp. 478-483.
27. D. Kumar Sahoo, R.K. Lal, H. Kim, V. Tilak, and L.F. Eastman, "High-field effects in silicon nitride passivated GaN MODEFTs," *IEEE Transactions on Electron Devices*, vol. 50, no. 5, 2003, pp. 1163-1170.
28. A.M. Conway, M. Chen, P. Hashimoto, P.J. Willadsen, and M. Micovic, "Failure Mechanisms in GaN HFETs under Accelerated RF Stress," *CS MANTECH Conference*, May 14-17, 2007, Austin Texas.
29. N. Ikeda, S. Kaya, J. Li, Y. Sato, S. Kato, S. Yoshida, "High power AlGaIn/GaN HFET with a high breakdown voltage of over 1.8KV on 4 inch Si substrate and suppression of current collapse," *Proceedings of the 20th International Symposium on Power Semiconductor Devices and ICs*, 2008, pp. 287-290.
30. V. Kumar, A. Kuliev, T. Tanaka, Y. Otoki, I. Adesida, "High transconductance enhancement-mode AlGaIn/GaN HEMTs on SiC substrate," *Electronics Letters*, vol. 39, no. 24, 2003, pp. 1758-1760.
31. Y. Cai, Y. Zhou, K. J. Chen, K. M. Lau, "High Performance Enhancement-Mode AlGaIn/GaN HEMT Using Fluoride-Based Plasma Treatment," *IEEE Electron Device Letters*, vol. 26, no. 7, 2005, pp. 435-437.

Appendix

APPENDIX I:	Product Matrix Table
APPENDIX II:	Reliability Test Table
APPENDIX III:	Reliability Results Table
APPENDIX IV:	HTRB Results
APPENDIX V:	HTGB Results
APPENDIX VI:	TC Results
APPENDIX VII:	THB Results
APPENDIX VIII:	Power Supply Operating Life Results

Appendix I: Product Matrix Table

Part Number	Voltage Rating	R _{DS(on)} Max	Package Dimensions
	(V)	(mΩ)	(mm x mm)
EPC1014	40	16	LGA 1.7 x 1.1
EPC1015	40	4	LGA 4.1 x 1.6
EPC1009	60	30	LGA 1.7 x 1.1
EPC1005	60	7	LGA 4.1 x 1.6
EPC1007	100	30	LGA 1.7 x 1.1
EPC1001	100	7	LGA 4.1 x 1.6
EPC1013	150	100	LGA 1.7 x 0.9
EPC1011	150	25	LGA 3.6 x 1.6
EPC1012	200	100	LGA 1.7 x 0.9
EPC1010	200	25	LGA 3.6 x 1.6

Appendix II: Reliability Test Table

Reliability Stress Test	Applicable Standard	Product	Stress Conditions
High Temperature Reverse Bias (HTRB)	JEDEC Std JESD22-A108	EPC1001, EPC1014	100% rated drain bias, 125°C
High Temperature Gate Bias (HTGB)	JEDEC Std JESD22-A108	EPC1001	5 V, 5.4 V, 6 V gate bias, 125°C
Temperature Cycling (TC)	JEDEC Std JESD22-A104	EPC1001, EPC1014	-40°C to 125°C, 2 cycles per hour
Temperature Humidity Bias (THB)	JEDEC Std JESD22-A101	EPC1014	85°C/85 RH, rated drain bias or max 100 V drain bias
Power Supply Operating Life		EPC1001	10 A, 250 kHz, 30°C

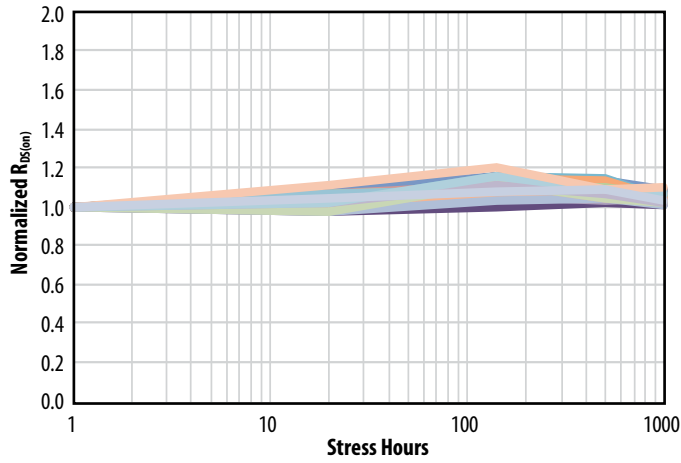
Appendix III: Reliability Results Table

Stress Test	Part Number	Sample Size	# of Fail at Read Point			
			24 HR	168 HR	500 HR	1000 HR
HTRB	EPC1001	45	0	0	0	0
HTRB	EPC1014	50	0	0	0	0
Stress Test	Part Number	Sample Size	# of Fail at Read Point			
			24 HR	168 HR	500 HR	1000 HR
HTGB 5 V	EPC1001	45	0	0	0	0
HTGB 5.4 V	EPC1001	45	0	0	0	0
HTGB 6 V	EPC1001	50	0	5*		
Stress Test	Part Number	Sample Size	# of Fail at Read Point			
			48 cys	168 cys	500 cys	1000 cys
TC	EPC1001	45	0	0	0	0
TC	EPC1014	50	0	0	0	0
Stress Test	Part Number	Sample Size	# of Fail at Read Point			
			24 HR	168 HR	500 HR	1000 HR
THB	EPC1014	45	0	0	0	
Stress Test	Part Number	Sample Size	# of Fail at Read Point			
			24 HR	168 HR	500 HR	1000 HR
Power Supply Life Test	EPC1001	10	0	0	0	0

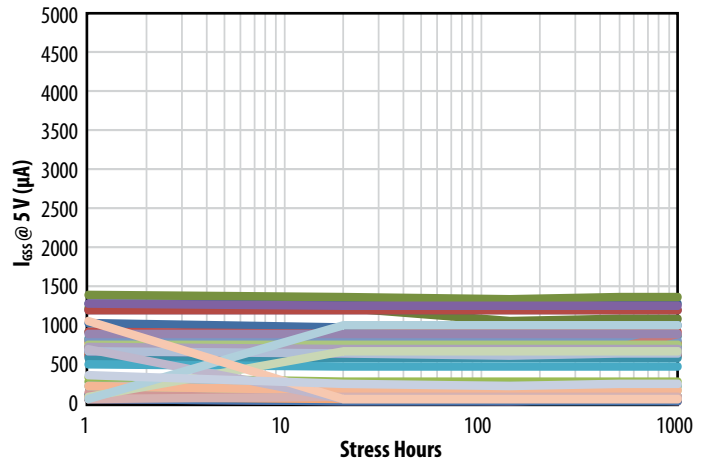
Appendix IV: HTRB Maximum Rated Voltage at 125°C

EPC1001 HTRB 100 V at 125°C

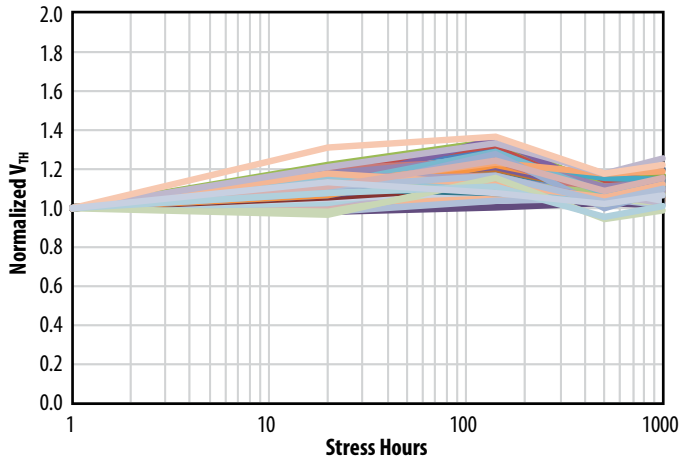
HTRB EPC1001 $R_{DS(on)}$ vs. Stress Time



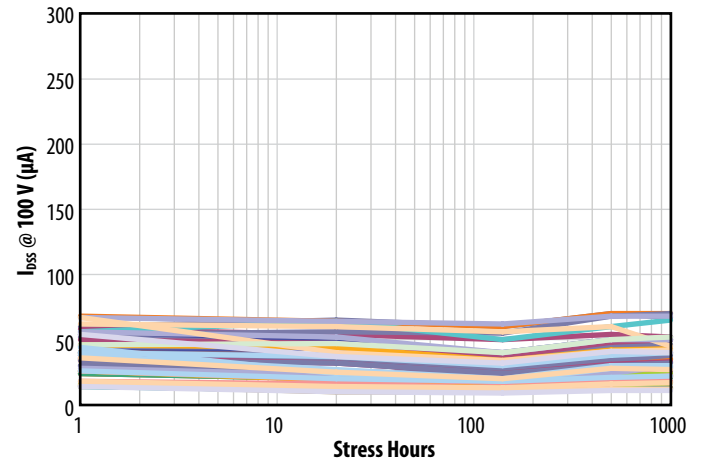
HTRB EPC1001 $I_{GSS} @ 5 V$ vs. Stress Time



HTRB EPC1001 V_{TH} vs. Stress Time

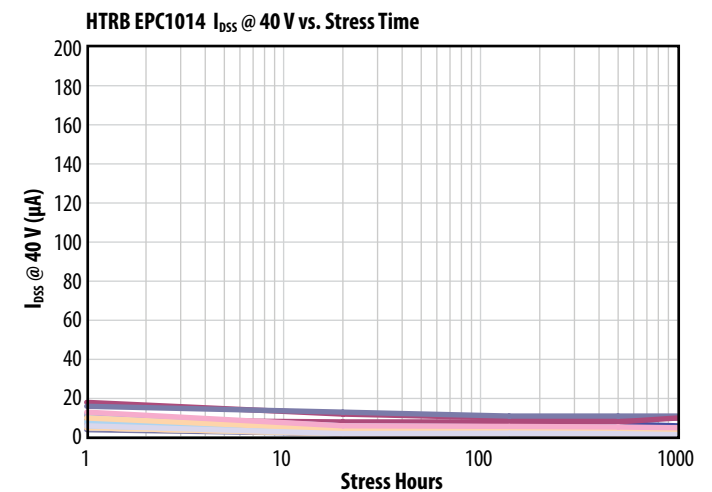
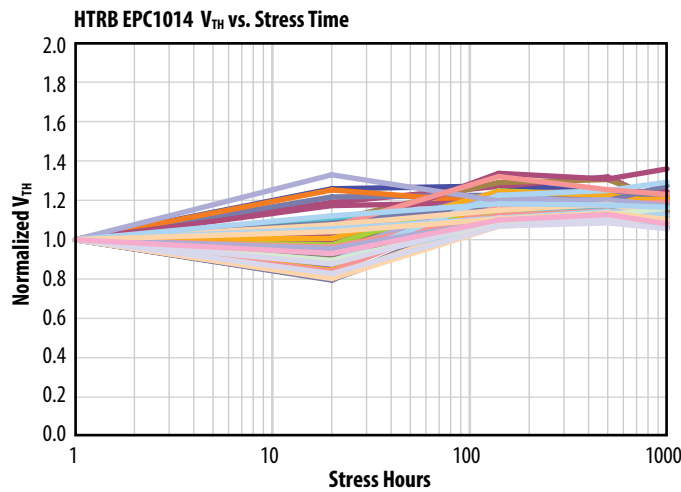
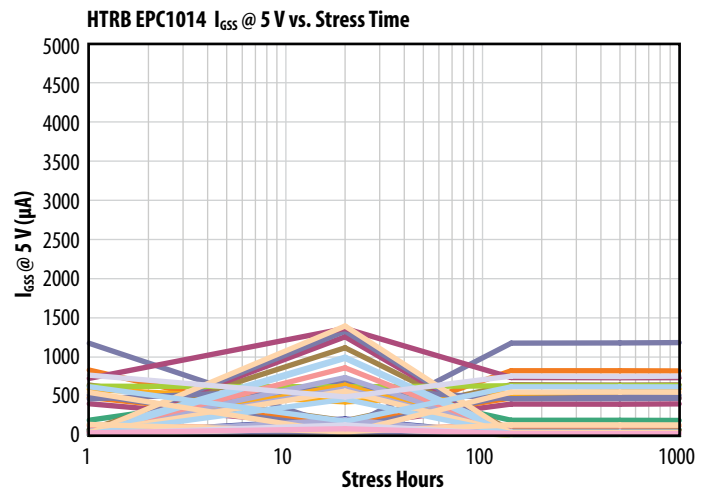
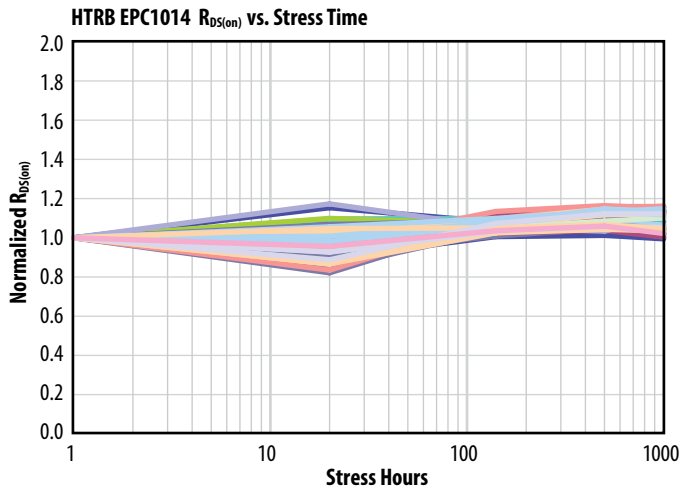


HTRB EPC1001 I_{DSS} vs. Stress Time



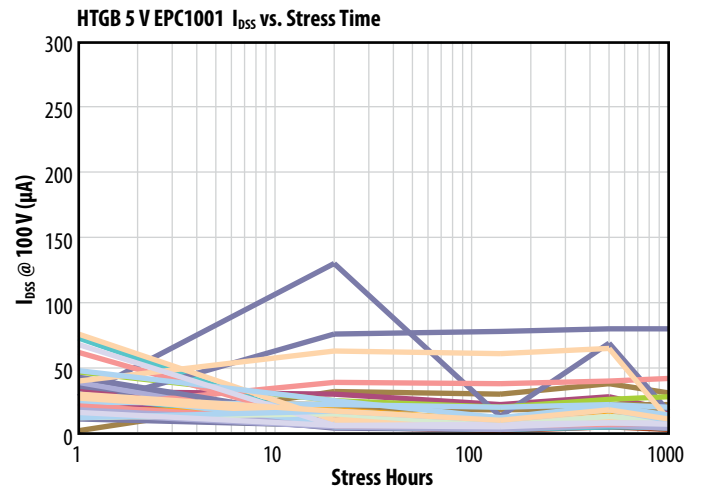
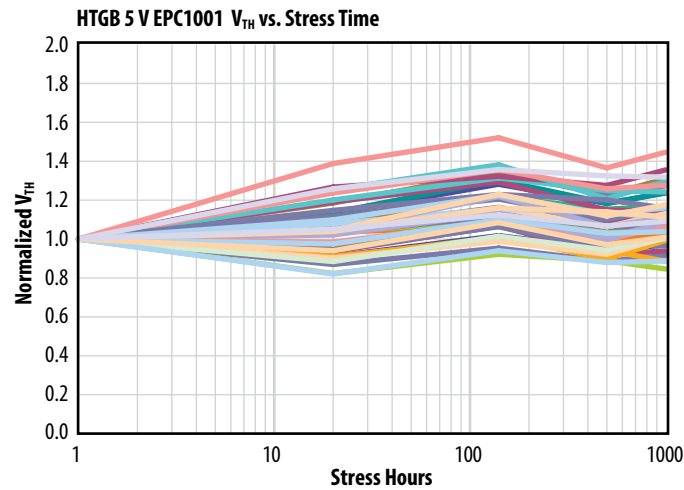
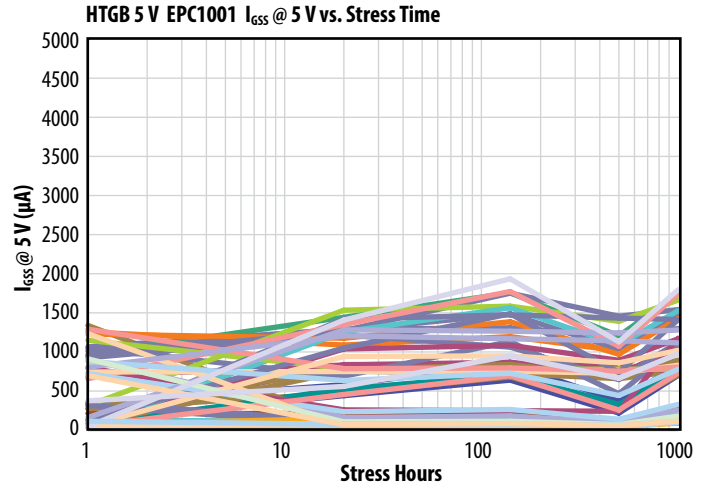
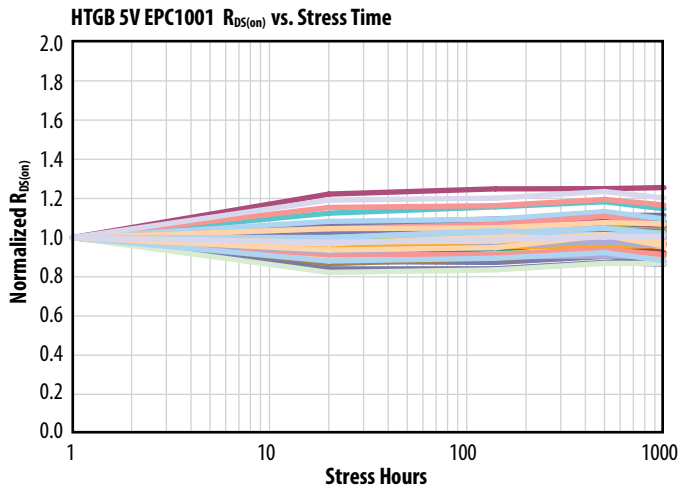
Appendix IV: HTRB Maximum Rated Voltage at 125°C

EPC1014 HTRB 40 V at 125°C



Appendix V: HTGB @ 125°C

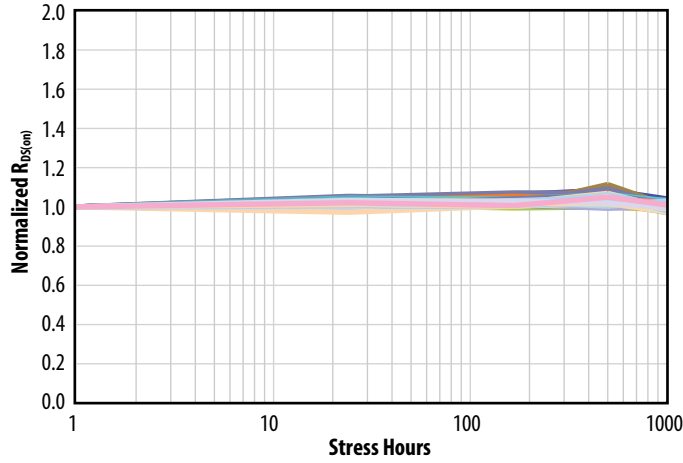
EPC1001 HTGB 5 V at 125°C



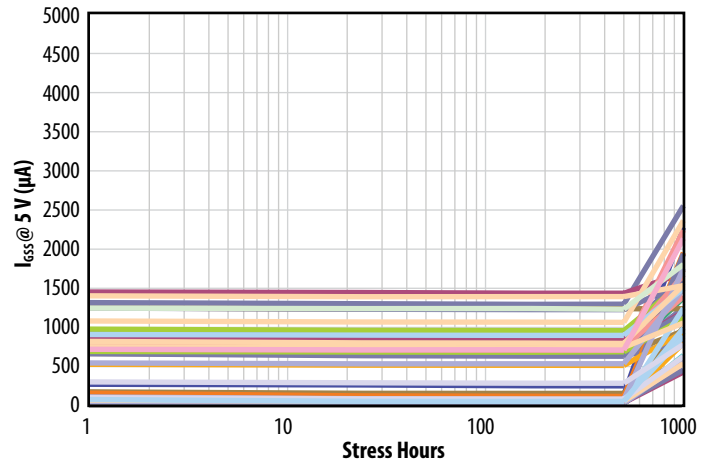
Appendix V: HTGB @ 125°C

EPC1001 HTGB 5.4 V at 125°C

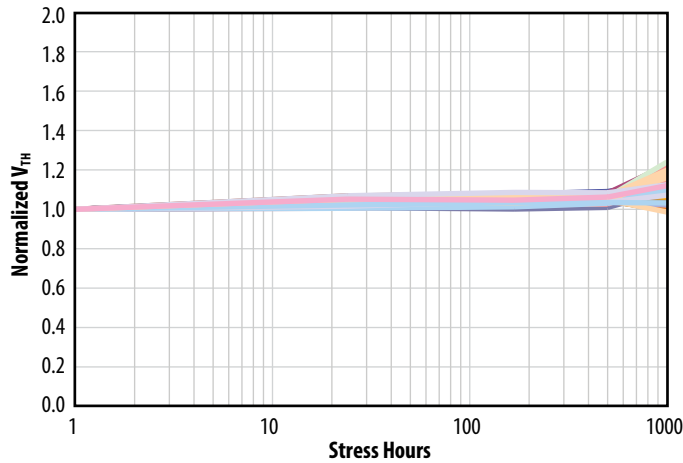
HTGB 5.4 V EPC1001 $R_{DS(on)}$ vs. Stress Time



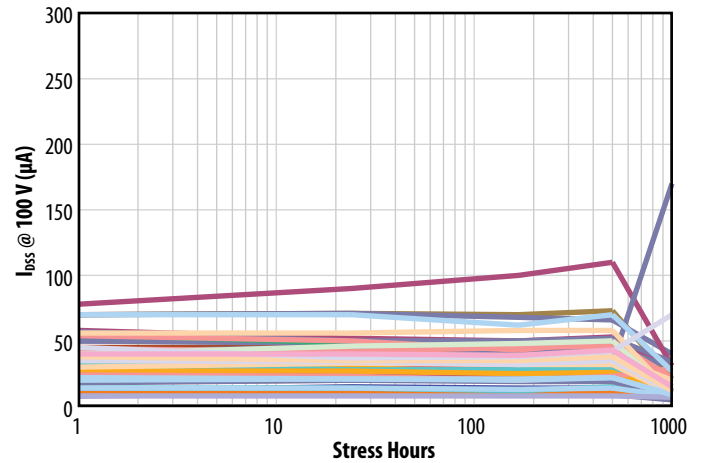
HTGB 5.4 V EPC1001 $I_{GSS@5V}$ vs. Stress Time



HTGB 5.4 V EPC1001 V_{TH} vs. Stress Time

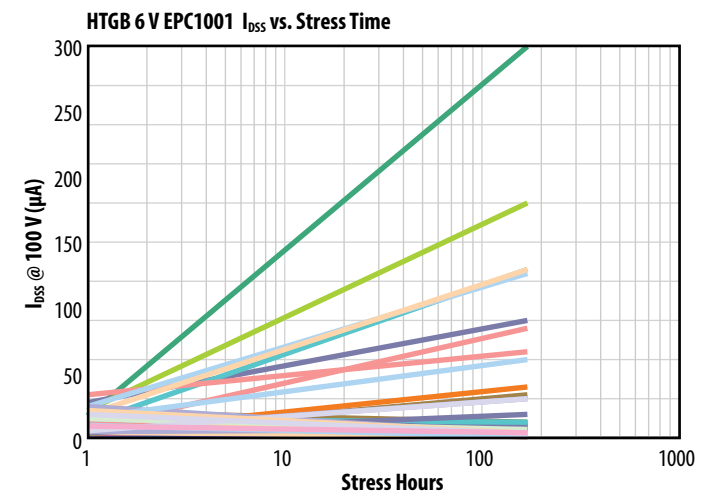
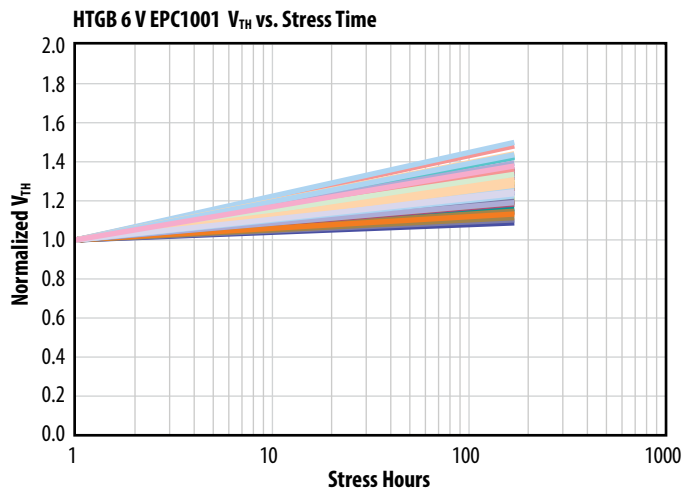
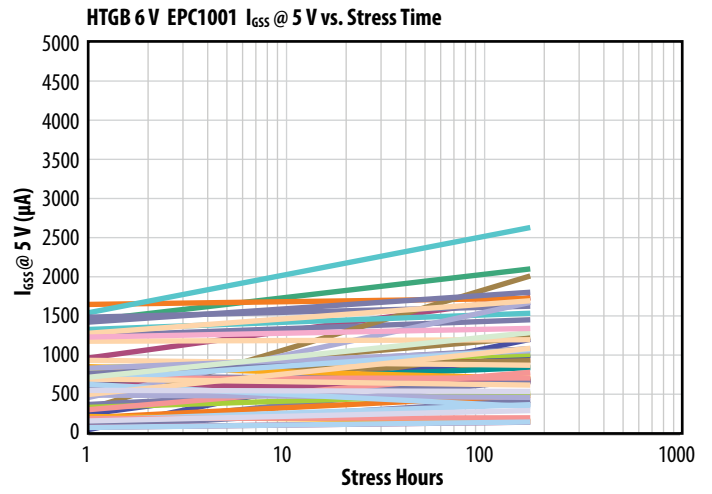
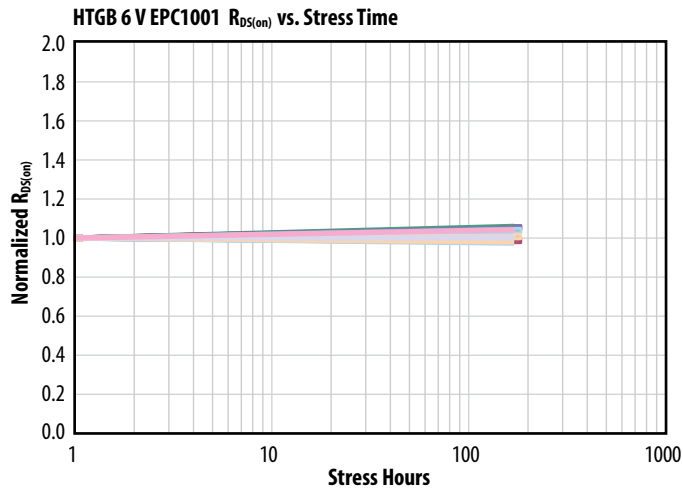


HTGB 5.4 V EPC1001 I_{DSS} vs. Stress Time



Appendix V: HTGB @ 125°C

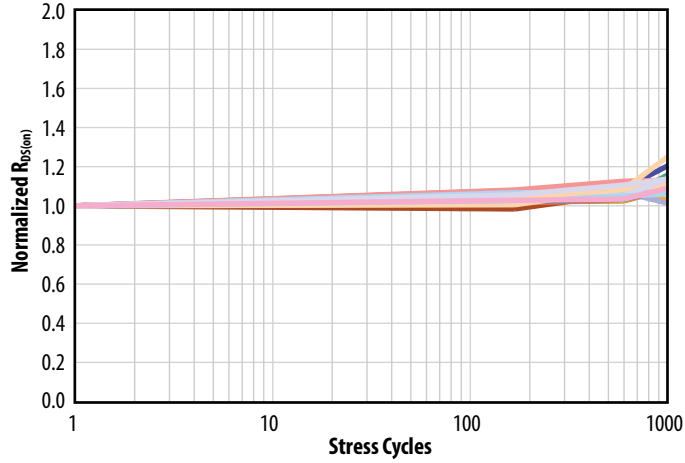
EPC1001 HTGB 6 V at 125°C



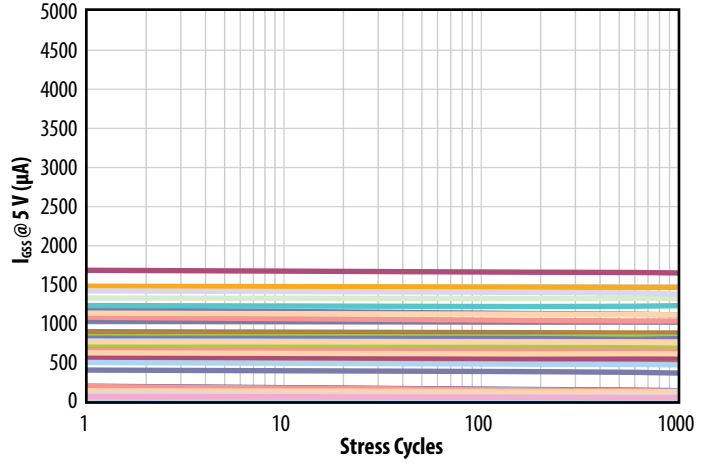
Appendix VI: Temperature Cycling -40°C to 125°C

EPC1001 TC -40°C to 125°C

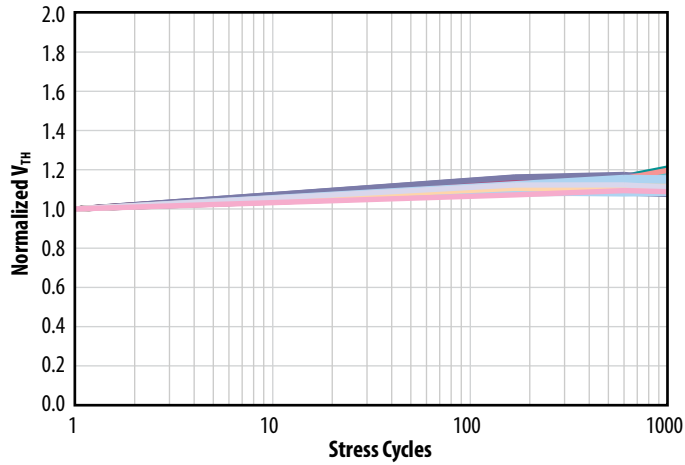
TC EPC1001 $R_{DS(on)}$ vs. Stress



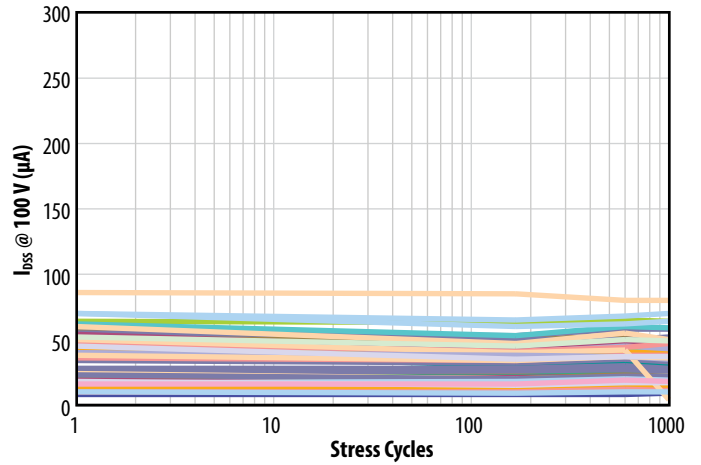
TC EPC1001 $I_{GSS @ 5V}$ vs. Stress



TC EPC1001 V_{TH} vs. Stress



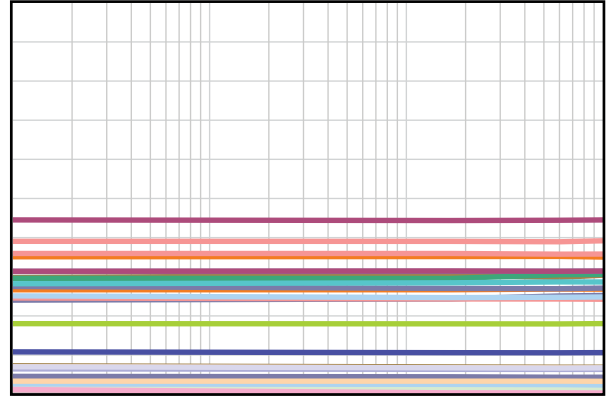
TC EPC1001 I_{DSS} vs. Stress



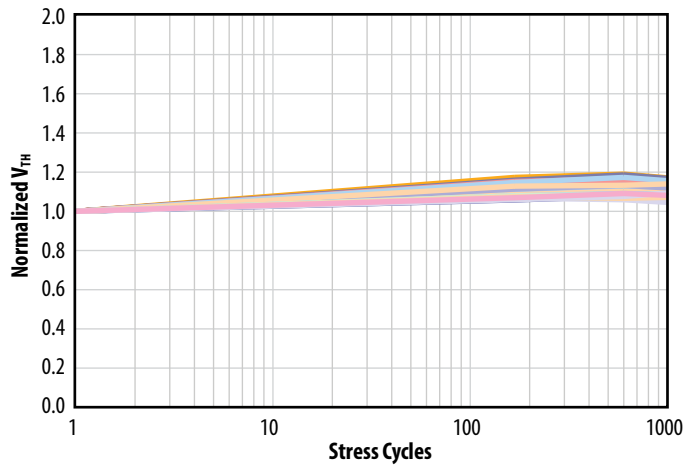
Appendix VI: Temperature Cycling -40°C to 125°C

EPC1014 TC -40°C to 125°C

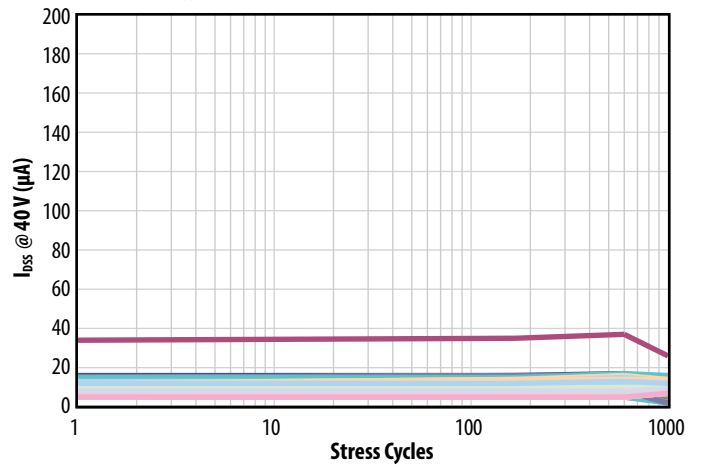
TC EPC1014 $R_{DS(on)}$ vs. Stress



TC EPC1014 V_{TH} vs. Stress



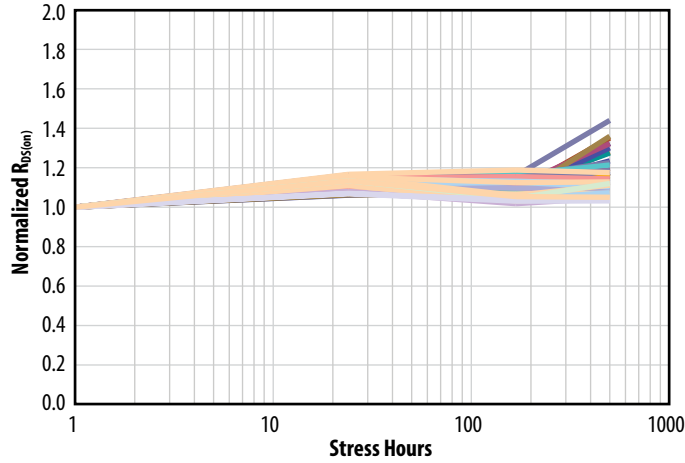
TC EPC1014 I_{DSS} vs. Stress



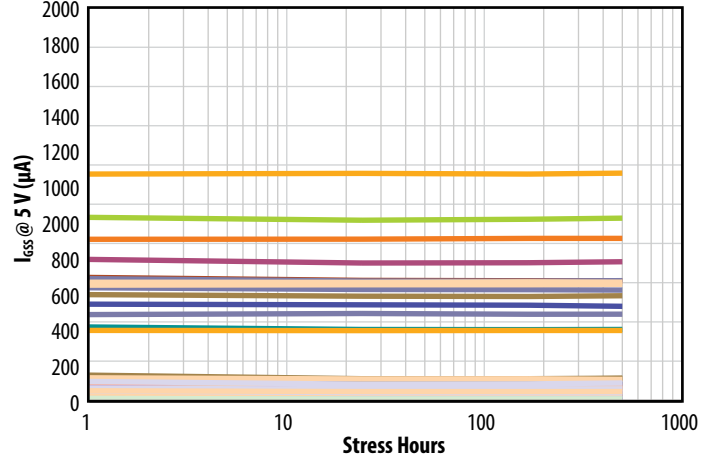
Appendix VII: THB 85°C, 85% RH

EPC1014 THB 85°C / 85 RH 40 V

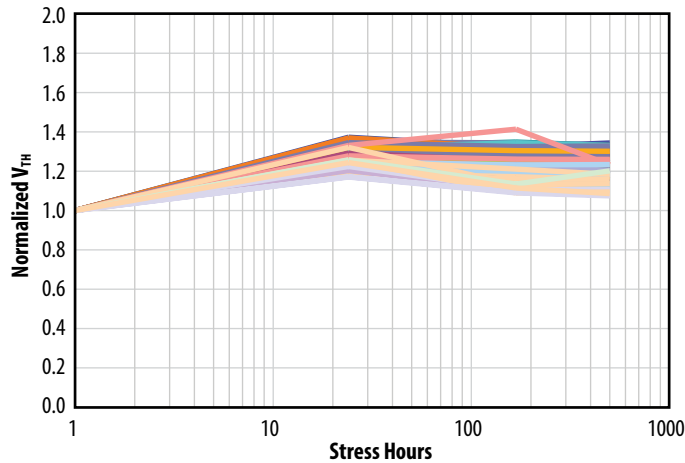
THB EPC1014 $R_{DS(on)}$ vs. Stress Time



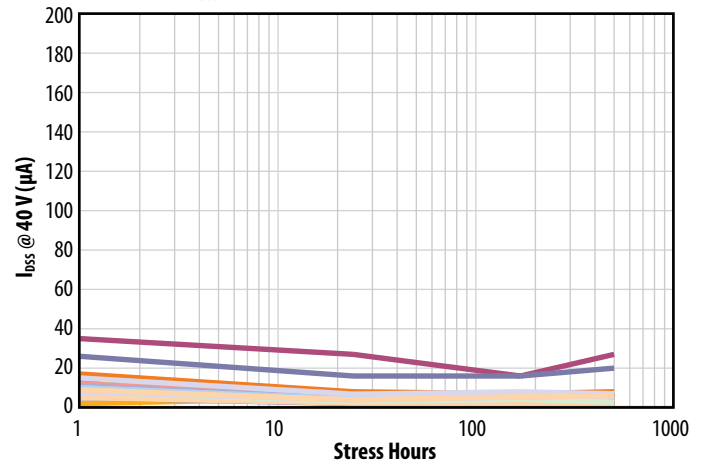
THB EPC1014 $I_{GSS @ 5 V}$ vs. Stress Time



THB EPC1014 V_{TH} vs. Stress Time



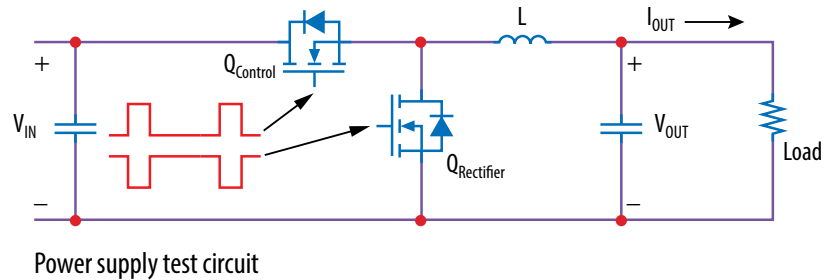
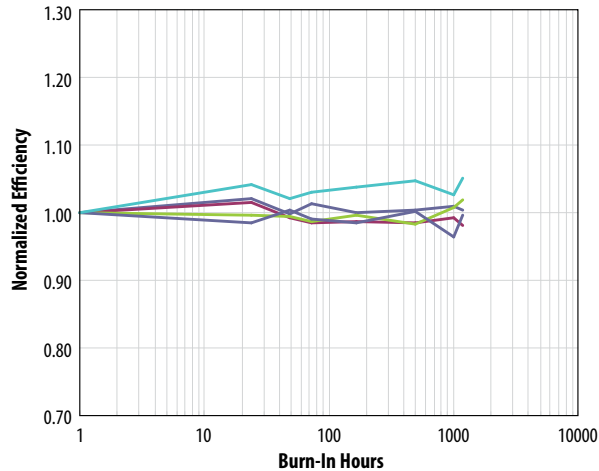
THB EPC1014 $I_{DSS @ 40 V}$ vs. Stress Time



Appendix VIII: Operating Life Tests

EPC1001 Power Supply Operating Life

$48 V_{IN} - 1 V_{OUT}$, 10 A Load, 250 kHz



For More Information:

Please contact info@epc-co.com
or your local sales representative

Visit our website:
www.epc-co.com

Sign-up to receive
EPC updates at
bit.ly/EPCupdates
or text "EPC" to 22828



EPC Products are distributed through Digi-Key.
www.digikey.com